GASEOUS RESPONSE TO BAR-LIKE DISTORTIONS

William W. Roberts, Jr.
University of Virginia

In this review the large-scale dynamics of the gas in a model disk galaxy which has an oval, bar-like distortion (or bar structure) in the inner parts is reviewed from the standpoint of recent gas dynamical studies, both steady state and time evolutionary.

GALACTIC SHOCKS AND LARGE NONCIRCULAR MOTIONS

In the early 1960s Prendergast already suspected that the narrow dark dust lanes observed along the bar structure in barred spirals, such as NGC 1300 shown in Figure 1, may be related to galactic shocks formed within the gas (Prendergast, 1962). This suspicion together with the early work of Lin and Shu (1964, 1966) on the density wave picture of spiral structure motivated the steady state gas dynamical studies of the late 1960s (Fujimoto, 1968; Roberts, 1969; Roberts and Yuan, 1970) in which the gaseous response to a spiral perturbation gravitational field underlying a spiral density wave pattern was found to be strong and cap-able of inducing the formation of large-scale shock waves along the spiral arms. These studies identified the dark dust lanes along spiral arms as possible tracers of shocks and the galactic shock itself as a possible triggering mechanism for the formation of young stellar associations and H II regions "strung out like pearls along the arms" (Baade, 1963).
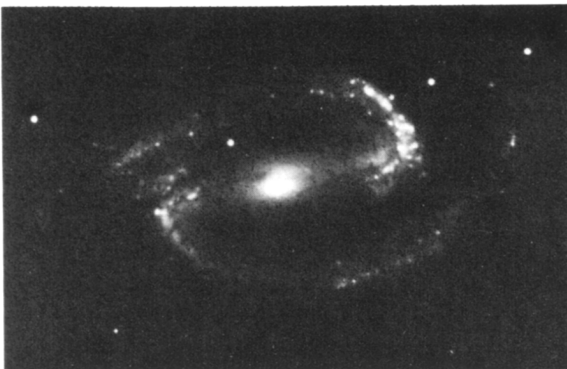

Figure 1. Photograph of the barred spiral galaxy NGC 1300 (The Hale Observatories).

175

The steady state response of the gas to a mild <u>bar-like</u> distortion
rotating at a small angular speed Ω_p was considered by Roberts (1971).
Figure 2 shows the equipotential contours of the nonaxisymmetric gravita-
tional field. The remarkably strong gaseous response driven by this weak-
ly perturbed field is shown in Figure 3. Galactic shocks form in lanes
slightly offset along the major axis of the bar-like distortion. These
offset shocks together with the highly oval gas streamlines, large noncir-
cular motions, and strong radial gas streaming along the bar, all driven
in the presence of only weak forcing, provided a nice preview as early as
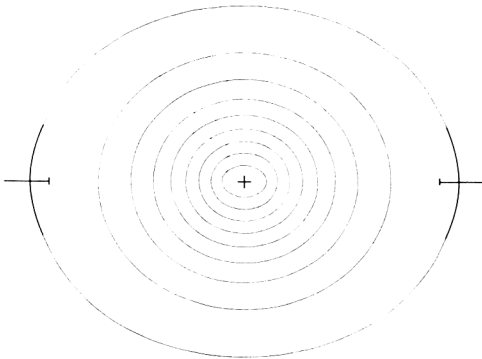1971 of what was to come in later work.

Figure 2. Equipotential con-
tours in a model disk galaxy
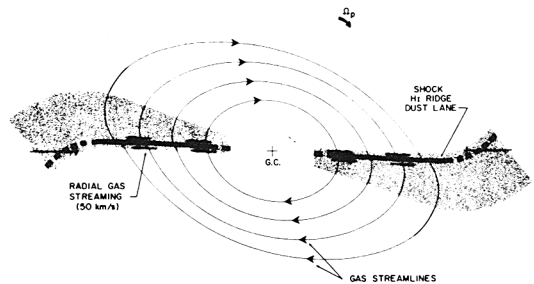with a mild (10%) bar-like
distortion (Roberts, 1971).

Figure 3. Oval steady state gas circula-
tion driven by the gravitational field of
the bar-like distortion in the model disk
galaxy (Fig. 2). Galactic shocks and
large noncircular motions characterize
the flow (Roberts, 1971).

THE "3 KPC ARM" FEATURE

Evidence for the existence of a weak bar structure in the inner parts
of our Galaxy has been discussed by de Vaucouleurs (1964, 1970) and by
Kerr (1967). Figure 4 shows the observed 21-cm velocity longitude map as
derived by Peters (1975) from Kerr's (1969) 21-cm survey, galactic equator
scan. The dark curve labelled ① traces the "3 kpc arm" feature. The
first inkling that the "3 kpc arm" feature could result from the gaseous
response to a bar-like distortion comes from Peters (Peters and Roberts,
1972) who takes the dynamical model of Roberts (1971, see Figure 3) with-
out any changes and views it at various orientations with respect to the
galactocentric line. The 21-cm line profiles which would be observed in
our Galaxy from neutral hydrogen having the velocity and density distribu-
tions predicted in the model are determined over the longitude range:
$-20°$ to $20°$. The results give a "3 kpc arm" feature for an orientation
of the oval streamlines at about $135°$ measured counterclockwise from the
galactocentric line. What is remarkable: the comparison with the observ-
ed "3 kpc arm" feature shows surprisingly good agreement in view of the
fact that the orientation is the only parameter adjusted. What is strik-
ing: this "3 kpc arm" feature is produced not from gas of high density,

as in a real spiral arm, but rather from less dense gas integrated over
large distances along the line of sight over the oval annular region along
and between streamlines. Figure 5 shows the predicted 21-cm velocity
longitude map derived in the subsequent work of Peters (1975) in which he
relaxes his dependence on the dynamical model in an attempt to account for
additional features, to the extent of kinematically modelling with smooth-
ed ellipses and allowing freedom in the choice of two parameters - the
axial ratio and the mean angular momentum/unit mass - as functions of
radius. Other attempts to account for the "3 kpc arm" feature are made by
Simonson and Mader (1972, 1973) with an elliptical dispersion ring model
and by Sanders and Prendergast (1974) with a nuclear explosion model.
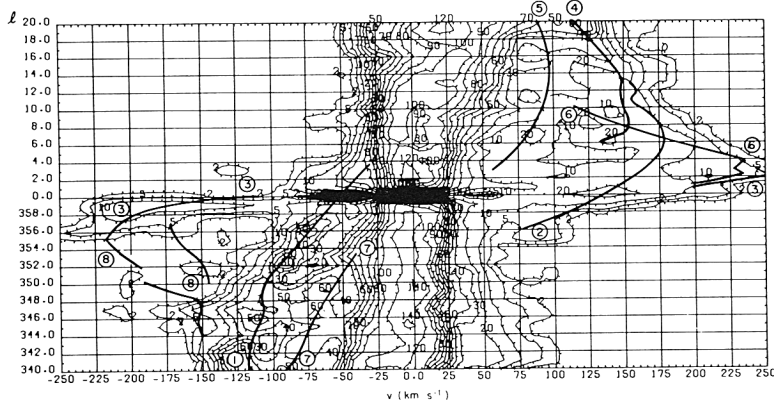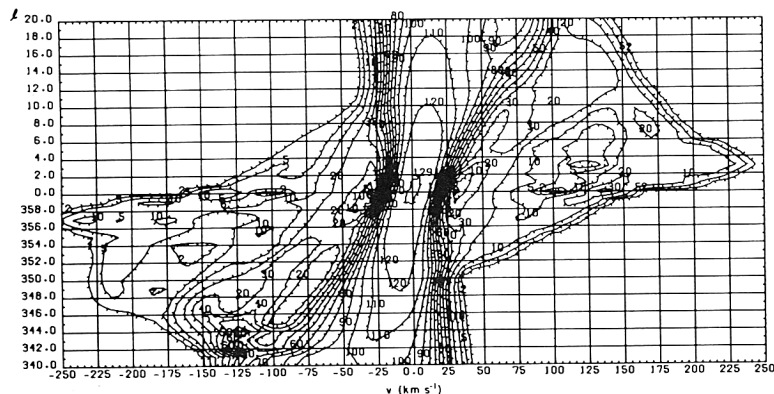

Figure 4.

Figure 5.

Figure 4. Observed 21-cm velocity longitude map derived from Kerr's (1969)
21-cm survey, galactic equator scan. The solid curves, also from Wester-
hout's (1969) survey. Curve ① - "3 kpc arm" feature (Peters, 1975).
Figure 5. Predicted 21-cm velocity longitude map derived from a kinematic
elliptical flow model not greatly different from the dynamical, oval circu-
lation model driven by a bar-like distortion (Figure 3). (Peters, 1975)

STEADY STATE GAS FLOW

     Roberts and Huntley (1978; also see Roberts, Huntley, and Lin, 1977)
generalize the steady state gas dynamical studies of the late 1960s for

tightly-wound normal spirals to include normal spirals with open spiral
arms and barred spirals with bar structures in the inner parts. The re-
sponse of the gas to a perturbing potential that is bar-like in the
interior and spiral-like in the exterior is calculated by means of an
analysis which enables the two-dimensional flow to be broken up into two
physical regimes, illustrated in Figure 6. In regime I near and within
the bar (and spiral arms), the flow is determined through an asymptotic
approximation that neglects the small variation of the velocity, density,
and pressure along a shock with respect to that variation normal to the
shock. In regime II where the flow is highly supersonic, the flow is
determined through an asymptotic approximation that neglects secondary
terms proportional to the square of the dispersion speed, such as the
transverse gradient of pressure. The composite picture for the steady
state flow of gas is constructed by joining the two regimes of flow in
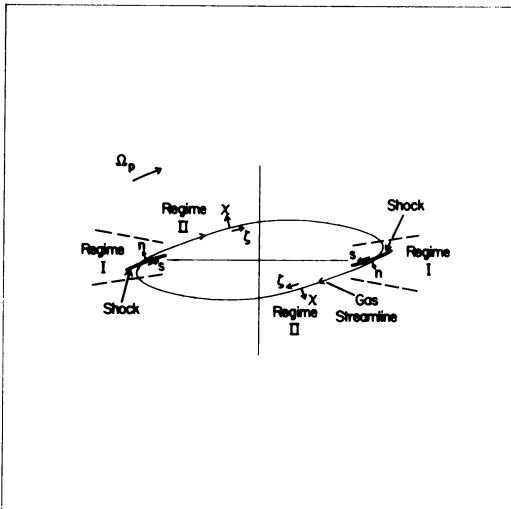the transition layer between regimes.

Figure 6. Schematic of the
steady state flow along a
streamline, and the locations
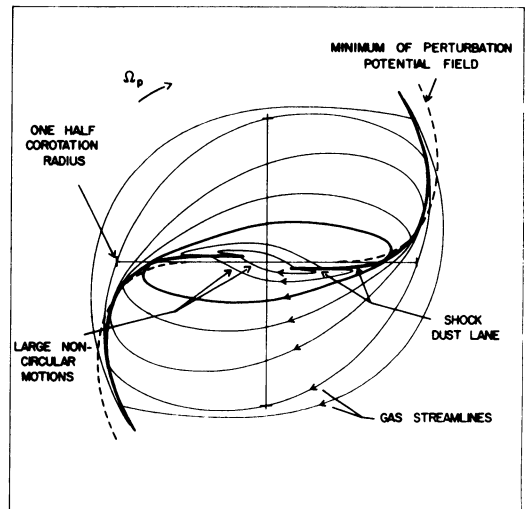of regimes I and II (Roberts
and Huntley, 1978).

Figure 7. Oval steady state gas circu-
lation in a Toomre model with a spheroid-
al component, driven by a mild bar-like
distortion. In the inner parts the re-
sponse shows offset shocks, large noncir-
cular motions (50-100 km/s), and radial
gas streaming (Roberts and Huntley, 1978).

     This composite picture is shown in Figure 7 for the case of a thin
disk Toomre (1963) model with a spheroidal component superposed in the
inner parts and a perturbing potential representing a 6% perturbation.
Galactic shocks are present, and highly oval gas streamlines characterize
the circulation in the inner parts where large noncircular motions occur.
Strong velocity gradients are present across the major axis of the gas
bar near the shock. Because gas, in passage through an oblique shock,
must leave the shock at a more oblique angle than that angle at which it
entered, postshock gas in the bar region in the inner parts is directed
outwards whereas postshock gas in the spiral arm region in the outer parts

is directed inwards. This shock-focusing phenomenon, which focuses gas
in the inner parts outwards and gas in the outer parts inwards, leads to
enhanced concentrations of compressed gas in the region of convergence
where the spiral arm bends from the bar and may account in part for the
enhanced star formation activity observed at the ends of the bar structure
in many barred spirals.

Figure 8 shows why shocks form. The cusp-transition curve, for any
one of the four models shown, represents the critical level of forcing,
at any radius, for which the gas flow undergoes a transition from flow
without shocks to flow with shocks. The transition curve delineated with
solid round dots (——●——●——) represents the case of the Toomre model
with spheroidal component shown in Figure 7. The strong gaseous response
and the formation of shocks in this model result from the moderately-
strong (6%) forcing amplitude, here indicated by the horizontal dashed
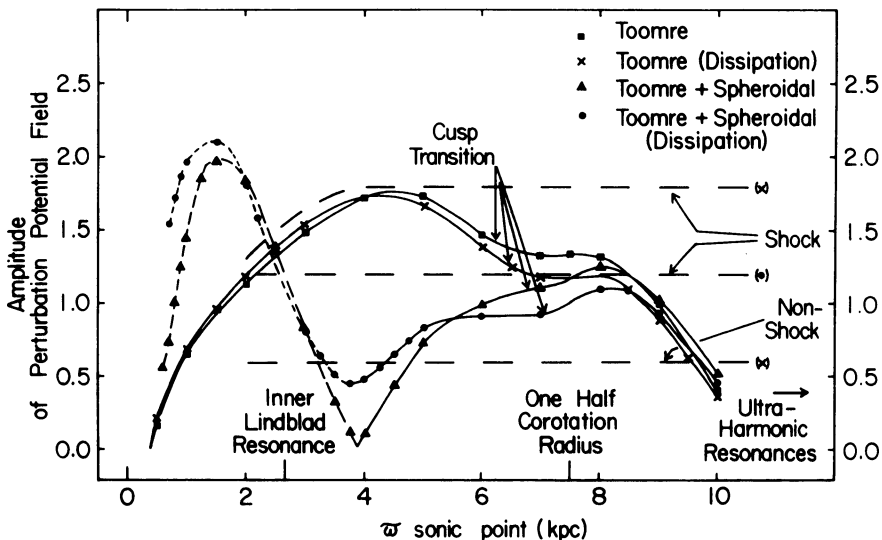line at A = 1.2, at a level above the transition curve.

Figure 8. Amplitude of the perturbation potential field of the bar-like
distortion which, at each radius, characterizes the transition from steady
state flow without shocks to steady state flow with shocks. A = 2.0 re-
presents a 10% perturbation (at ϖ = 5 kpc). (Roberts and Huntley, 1978)

TIME EVOLUTIONARY GAS FLOW

Time dependent, two-dimensional, numerical hydrodynamical calcula-
tions are carried out by Sanders and Huntley (1976), Sorensen, Matsuda,
and Fujimoto (1976), Huntley, Sanders, and Roberts (1978), and Liebovitch
(1978) for the time evolutionary response of gas to bar-like perturbations.
Sanders and Huntley for a power law disk model with a mild oval distortion
and Sorensen, Matsuda, and Fujimoto for an Eggen, Lynden-Bell, and Sandage
disk model with a strong prolate spheroidal distortion both found in 1976
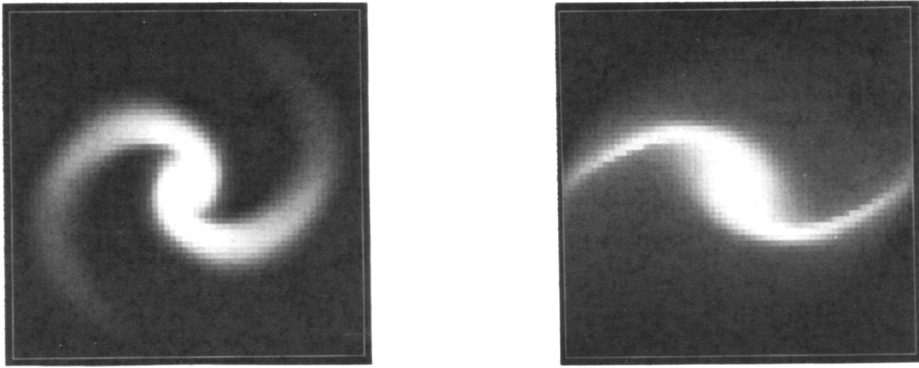the result that the time evolutionary gas response shows open trailing

Figure 9. Photographic simulation (a snapshot) of the time evolutionary
gas response in a power law disk model to a mild bar-like distortion for
two cases: left - inner and outer Lindblad resonance and corotation are
contained within the gaseous disk; right - only inner Lindblad resonance
is contained within the gaseous disk (Sanders and Huntley, 1976, as re-
calculated in the inertial frame by Huntley, 1977).

spiral density waves rotating with the angular speed of the distortion.
Figure 9 from Sanders and Huntley shows a photographic simulation of the
gas density distribution for the power law disk model as a snapshot in
time for two such cases. The shape of the spirals can be interpreted
through the coherent shifting in orientation of periodic particle orbits
between and across the resonances and corotation.

        Figure 10 from Huntley, Sanders, and Roberts for a Toomre model with
a mild bar-like distortion shows a gas response in the form of a prominent
central gas bar, with open trailing gaseous spiral density waves. Sanders
(1977) finds that the response of an ensemble of non-interacting test
particles to a bar-like distortion is bar-like, without appreciable spiral
arm formation; whereas when he repeats the calculation in a way in which
the test particles take on the character of a gas with an artificial vis-
cosity, he finds the response to be bar-like inside inner Lindblad reso-
nance, with two trailing spiral density waves outside. This result indi-
cates that the gaseous spiral density waves form through the dissipation
provided by the artificial viscosity in the numerical codes. Viscous
effects also induce a strong perennial inward drift of gas toward the
center.

Sorensen, Matsuda, and Fujimoto in their model with strong prolate spher-
oidal distortion find the time evolutionary response to be offset toward
the leading edges of the bar. With higher resolution, Huntley, Sanders,
and Roberts consider a similar case of a Toomre model with a prolate
spheroidal distortion, and a photographic simulation of this is shown in
Figure 11. The gas response in the inner parts is quite strong and shows
distinctly-offset lanes along the leading edges of the underlying bar-like
prolate spheroid. Of course there is still a problem of resolution,
directly related to the smoothing effects of artificial viscosity in the
numerical code; nevertheless, it is tempting to identify these offset
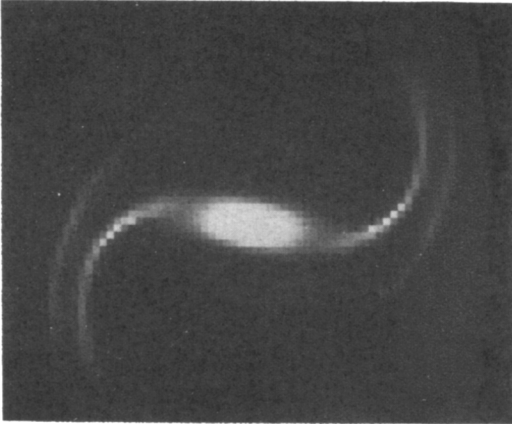features as tracers of large-scale shocks in the gas.

Figure 10. Photographic simulation
(a snapshot) of the time evolu-
tionary gas response in a Toomre
model to a mild bar-like distortion
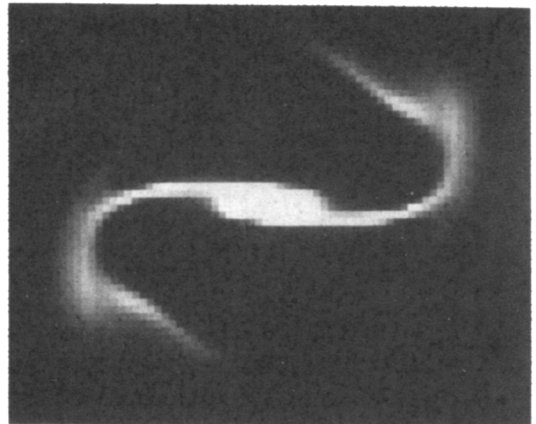(Huntley, Sanders, and Roberts,
1978).

Figure 11. Photographic simulation
(a snapshot) of the time evolu-
tionary gas response in a Toomre
model to a prolate spheroidal dis-
tortion (Huntley, Sanders, and
Roberts, 1978).

In order to focus in more detail on these features, we will return
to the steady state model (Figure 7) where viscous smoothing does not
enter. Figure 12 shows the velocity field for this steady state model
in a display which plots velocity vectors at approximately 6400 cell
positions over an 80 by 80 grid, 1 cell/300 pcs here, which is the identi-
cal grid size used in the time evolutionary calculations. Numerous arrows
delineate the strong outward preshock flow approaching the shock and also
the strong inward postshock flow at distances downstream from the shock.
Only two arrows are apparent which delineate the outward, highly oblique
postshock flow just adjacent to the shock. Corresponding velocity field
displays for the time evolutionary calculations show a strikingly similar
character; except in the narrow postshock region just adjacent to the
shock, not even one arrow can be found which delineates outward, highly
oblique postshock flow. The artificial viscosity is no doubt playing a
role in the time evolutionary calculations to smooth such fine features.
On the other hand the resolution of even the best, current observations
is coarser; and to that degree of resolution, such differences in the
theoretical displays would not even be detectable.

Recent time evolutionary, two dimensional, numerical calculations by
Liebovitch (1978) on the gas response to an imposed perturbing potential
that is bar-like in the interior and spiral-like in the exterior, on a
polar coordinate grid, provide important confirmations of many of the
results found in these earlier studies. Liebovitch confirms such effects
as the offsetness of the gas features along the bar. Figure 13 shows his
determination of the clockwise phase shift toward 90° of the gas bar rela-
tive to the (horizontal) driving bar, for the case of a disk model with
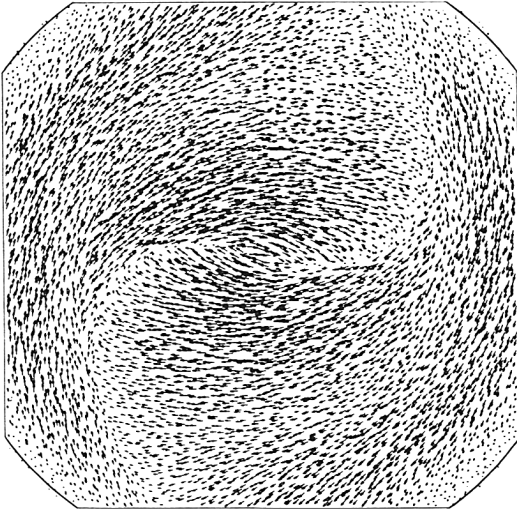one inner Lindblad resonance when the amplitude of the driving bar is

Figure 12. Velocity field of the
steady state model in Figure 7,
delineated by some 6400 velocity
vectors. To this degree of reso-
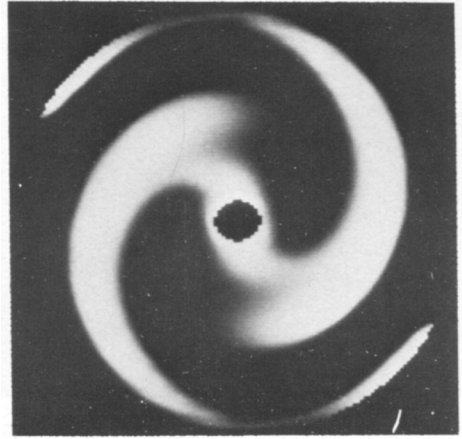lution, shocks are detectable
(Roberts and Huntley, 1978).

Figure 13. Photographic simulation
of the gas density distribution for
a case in which the gas bar response
shifts to approximately 90^0 out of
phase with the driving bar
(Liebovitch, 1978).

reduced toward zero. In addition, he finds broad appendages of high gas
density that extend past the bend where the central bar bends into spiral
arms (most likely related to the shock-focusing phenomenon discussed
earlier); and these he associates with the bright appendages to the
spiral arms seen in many barred spirals.

A SAMPLE BARRED SPIRAL

        One of the most detailed velocity field maps for barred spirals
available to date in the literature is that of NGC 5383 (photograph
shown in Figure 14) derived from spectroscopic observations by Peterson,

Figure 14. Photograph of
the barred spiral galaxy
NGC 5383 (The Kitt Peak
National Observatory).
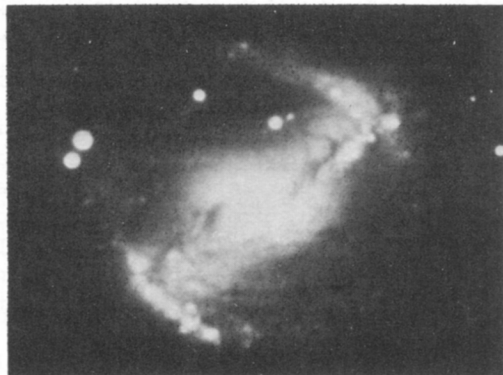
Rubin, Ford, and Thonnard (1978). Figure 15 shows this observed velocity
field map. Probably what is most striking: the strong velocity gradient
across the bar, as evidenced by the crowding of isovelocity contours there
Such a strong velocity gradient may be directly related to the bar-driven
flow of gas in NGC 5383.

    In order to investigate this possibility we will adopt the steady
state model (Figures 7 and 12) and view it in the same orientation as
NGC 5383 is viewed in the sky. Figure 16 from Roberts and Huntley (1978)
shows the velocity field map (solid lines) predicted from the steady state
model; independently Huntley (1978) has followed a similar procedure for
a time evolutionary model. As in the observed map, what is most striking
in Figure 16 is the strong gradient of velocity across the bar, which in
the model is a result of the highly oval gas circulation driven by the
bar-like potential field. Overall there seems to be general agreement
between these isovelocity contours and those in the observed map. Perhaps
of further interest is the trough in the -50 and -100 km/s isovelocity
contours in the NW quadrant where these contours cross the shock and
spiral arm, and also the corresponding trough in the 50 and 100 km/s
isovelocity contours in the SE quadrant. Similar troughs show up in the
observed map in the -100 and 100 km/s isovelocity contours in the regions
where these contours cross the arms near the ends of the bar. If further
observations of this type could be made, particularly near and along the
bar structure and spiral arms, corresponding troughs and other detailed
variations in more of the observed isovelocity contours might be detect-
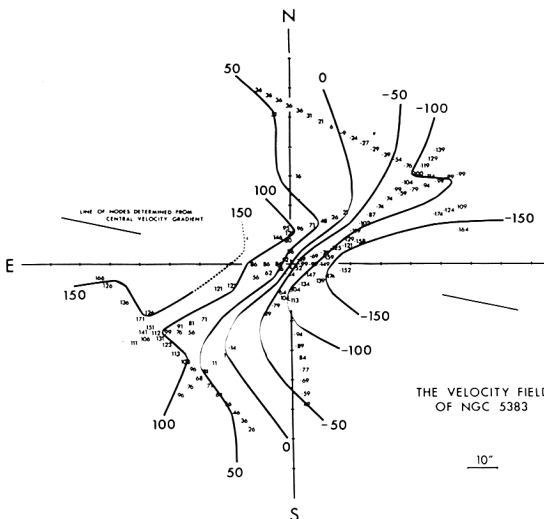able and help to further reflect the underlying dynamics.

Figure 15. Observed velocity field
of the barred spiral galaxy NGC 5383
characterized by a strong gradient
in velocity across the bar
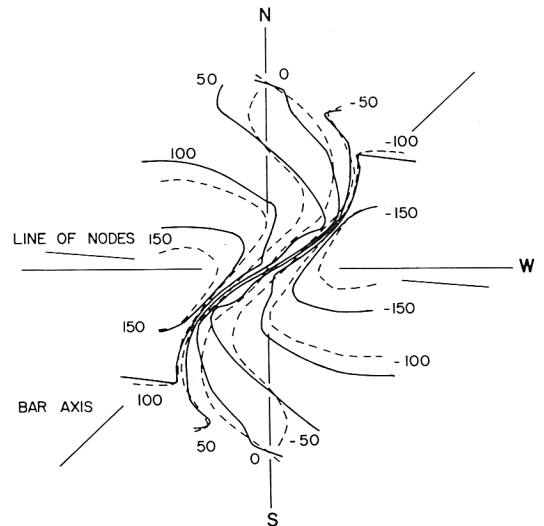(Peterson, Rubin, Ford, and
Thonnard, 1978).

Figure 16. Predicted velocity field
of the steady state model in Figures
7 and 12, with the same orientation
as that observationally-derived for
NGC 5383 (Roberts and Huntley, 1978).

OUR GALAXY - NOT A BIRD'S EYE VIEW

Does our Galaxy contain a bar-like distortion or bar structure in the inner parts? If so, how prominent is it and what characteristics does it share in common with the bar structures in NGC 1300 or NGC 5383 or other external barred spirals which we see with a bird's eye view? Perhaps the results and implications of the studies reviewed herein will motivate future studies, both observational and theoretical, to help us focus further on this intriguing question, toward a deeper understanding of our Galaxy.

REFERENCES

Baade, W., 1963, "Evolution of Stars and Galaxies," Harvard U., Cambridge.
de Vaucouleurs, G., 1964, in IAU Symp. No. 20, p. 195.
de Vaucouleurs, G., 1970, in IAU Symp. No. 38, p. 18.
Fujimoto, M., 1968, in IAU Symp. No. 29, p. 453.
Huntley, J. M., 1977, Ph. D. Thesis, U. of Va., Charlottesville.
Huntley, J. M., 1978, preprint.
Huntley, J. M., Sanders, R. H., Roberts, W. W., 1978, Ap. J., 221, p. 521.
Kerr, F. J., 1967, in IAU Symp. No. 31, p. 239.
Kerr, F. J., 1969, Australian J. Phys., Ap. Suppl., No. 9.
Liebovitch, L. S., 1978, Ph. D. Thesis, Harvard U., Cambridge.
Lin, C. C., and Shu, F. H., 1964, Ap. J., 140, p. 646.
Lin, C. C., and Shu, F. H., 1966, Proc. Natl. Acad. Sci., 55, p. 229.
Peters, W. L., 1975, Ap. J., 195, p. 617.
Peters, W. L., and Roberts, W. W., 1972, B.A.A.S., 4, p. 265.
Peterson, C. J., Rubin, V. C., Ford, W. K., Thonnard, N., 1978, Ap. J.,
      219, p. 31.
Prendergast, K. H., 1962, in Interstellar Matter in Galaxies,
      L. Woltjer (ed.), Benjamin, N. Y.
Roberts, W. W., 1969, Ap. J., 158, p. 123.
Roberts, W. W., 1971, B.A.A.S., 3, p. 369.
Roberts, W. W., and Huntley, J. M., 1978, Ap. J. (submitted for publ.).
Roberts, W. W., Huntley, J. M., Lin, C. C., 1977, in IAU Symp. No. 77.
Roberts, W. W., and Yuan, C., 1970, Ap. J., 161, p. 877.
Sanders, R. H., 1977, preprint.
Sanders, R. H., and Huntley, J. M., 1976, Ap. J., 209, p. 53.
Sanders, R. H., and Prendergast, K. H., 1974, Ap. J., 188, p. 489.
Simonson, S. C., and Mader, G. L., 1972, B.A.A.S., 4, 266.
Simonson, S. C., and Mader, G. L., 1973, Astr. and Ap., 27, p. 337.
Sorensen, S. A., Matsuda, T., and Fujimoto, M., 1976, Ap. Space Sci.,
      43, p. 491.
Toomre, A., 1963, Ap. J., 138, p. 385.
Westerhout, G., 1969, Maryland-Green Bank Galactic 21-cm Line Survey,
      2nd ed.

DISCUSSION

van den Bergh: Radio observations show that there is a small area
of very active star formation in the center of our Galaxy. In this re-
spect the Galaxy resembles external galaxies with nuclear hot spots.
About two-thirds of the objects with such hot spots are barred spirals.
This suggests that there is perhaps a 60% to 70% chance that the Galaxy
also contains a nuclear bar.

Contopoulos: I noticed (in one of your slides) that the streamlines
inside the bar are very elongated. According to my calculations this
should happen mainly near the Inner Lindblad Resonance. Where is the
Inner Lindblad Resonance in your model?

Roberts: In the steady-state model shown in Figure 7 of my paper,
highly oval gas streamlines occur in the vicinity of the Inner Lindblad
Resonance and in fact pass across this resonance region. In the (kpc)
units of Figures 7 and 8 the half co-rotation radius occurs at 7.5 kpc
(marked, and just outside the bend of the bar into spiral arms); the
Inner Lindblad Resonance, at 2.6 kpc; and the maximum and minimum radii
of the second innermost streamline, at 4.0 and 1.0 kpc, respectively.

Sanders: It seemed to me that in the steady-state calculations made by
you and Huntley the co-rotation radius was near the end of the bar; that
is, the bar is a fast bar. I know that with respect to the time depend-
ent calculations, it is certainly the case that co-rotation must lie
near the end of the bar in order to get reasonable offset shocks. Now
we lie in a region of spiral structure. This would suggest--if our
galaxy is a barred spiral like NGC 1300--we lie beyond co-rotation. On
the other hand, the fact that active star formation is occurring in the
region of the Sun implies that we lie inside co-rotation. This apparent
contradiction suggests to me that our Galaxy is not a barred spiral like
NGC 1300.

Roberts: I agree that a fast bar would result if co-rotation occurs as
far inwards as the radius at the ends of the bar. However, the bar in
NGC 1300 may not be so fast a rotator. First, the co-rotation radius
in the steady-state model, shown in my Figure 7, actually lies at the
outer edge of the disk outside the spirals; the bar is a slowly-rotating
bar, and the shocks occur offset with about the same offsetness as the
dark dust lanes observed along the bar in NGC 1300. Second, in the ob-
served photograph of NGC 1300 the dust lanes on the inner edges of the
spiral arms can be traced to a considerable radius; this implies that co-
rotation occurs outside this radius. These considerations do not sup-
port your chain of arguments. I believe that the evidence available
at this time does not rule out the possibility that our Galaxy may have
a bar or bar-like distortion like that of NGC 1300. However, I do agree
that such a bar or bar-like distortion in our Galaxy would probably be
a slow rotator.

Mark: Dr. Roberts showed that even a weak driving force in the form of
a bar plus open spiral would result in strong bar-like gas shocks. A
relevant question is whether or not the gas would react with strong
shocks to the modes we calculated which sometimes have the appearance
of an open spiral in the inner parts of the galaxy model. My guess is
that the gaseous response might not look like NGC 1300 because the per-
turbation densities and potentials do not reach the galactic center in
our modes. The situation could be different if the amount of bulge
matter is somewhat less than that used in our N-body simulation with
Bob Berman. In that case a weak bar or oval distortion forms in the
central regions and the gaseous response might indeed behave as in Dr.
Roberts' simulation.

Sanders: Let me elaborate on the point I made a minute ago about fast
bars. We have recently been investigating the gas response to bars by
means of time-dependent hydrodynamical calculations. The model for the
gravitational field consists of a homogeneous prolate spheroid embedded
in a disk. We have been exploring the parameter space of this model and
find that the gas response looks most similar to a barred spiral like
NGC 1300 whenever co-rotation lies just beyond the ends of the bar.
This is consistent with calculations made several years ago by
Prendergast which suggest that the location of the straight dust lanes
depend critically upon the presence of Lagrangian points near the ends
of the bar.

van Woerden: The pile up of gas just outside a bar may be seen well in
the barred Magellanic irregular NGC 4449. A Westerbork map of neutral
hydrogen in this galaxy (by Bosma and myself, in preparation) shows a
very strong ridge of hydrogen at the NE end of the bar, coinciding with
a chain of bright HII regions and associations.

de Vaucouleurs: I should like to call your attention to the on-going
program of Fabry-Perot interferometry at McDonald Observatory, includ-
ing many barred spirals. The first results will appear in the disser-
tation of W. Pence; this is a study of the velocity field in NGC 253
from about 10,000 individual velocities.

Roberts: I look forward to the publication of this high-resolution
study which perhaps can be compared with high-resolution theoretical
velocity-field maps, such as the one shown in my Figure 12, to help
guide future theoretical studies.